# Perpendicular magnetic anisotropy and high spin-polarization ratio in epitaxial Fe-N thin films

Nian Ji, M. S. Osofsky, Valeria Lauter, Lawrence F. Allard, Xuan Li, Kevin L. Jensen, Hailemariam Ambaye, Edgar Lara-Curzio, and Jian-Ping Wang

# Perpendicular magnetic anisotropy and high spin polarization ratio in epitaxial Fe-N thin films

Nian Ji[1,2], M. S. Osofsky[3], Valeria Lauter[4], Lawrence F. Allard[5], Xuan Li[1], Kevin L. Jensen[3], Hailemariam Ambaye[4] Edgar Lara-Curzio[5] and Jian-Ping Wang[1,2†]

[1]*The Center for Micromagnetics and Information Technologies (MINT) and Department of Electrical and Computer Engineering, University of Minnesota, Minneapolis, Minnesota 55455, USA*

[2]*Department of Physics University of Minnesota, Minneapolis, Minnesota 55455, USA*

[3]*Naval Research Laboratory, 4555 Overlook Ave SW, Washington, DC 20375, USA*

[4]*Spallation Neutron Source, Oak Ridge National Laboratory, Oak Ridge, Tennessee 37831, USA*

[5]*High Temperature Materials Laboratory, Oak Ridge National Laboratory, Oak Ridge, TN 37831, USA*

## Abstract

We have demonstrated a general framework for realizing and modulating perpendicular magnetic anisotropy in a *rare-earth-element and heavy-metal -free* material system. Using GaAs(001)/Fe(001) template, we have developed a synthesis scheme to produce epitaxial body center tetragonal Fe-N with (001) texture. By varying the N doping concentration, the crystal tetragonality (c/a) can be tuned in a relatively wide range. It is found that the Fe-N layer developed a strong perpendicular magnetic crystalline anisotropy (MCA) as it approaches the iron nitride interstitial solubility limit. Further annealing process significantly improves the MCA due to the formation of chemically ordered $Fe_{16}N_2$. In addition to realize an MCA up to $10^7$ erg/cm$^3$ , the spin polarization ratio (P~0.52), as probed directly by a Point Contact Andreev Reflection (PCAR) method, even shows a moderate increase in comparison with normal metal Fe (P~0.45). These combined properties make this material system a promising candidate for applications in spintronic devices and also potential rare-earth-element free magnets.

Key words: FeN, $Fe_{16}N_2$, $Fe_8N$, perpendicular anisotropy; spin polarization ratio; rare-earth-free magnet, spintronics, PCAR

1

# I.    INTRODUCTION

Giant magnetoresistive devices with perpendicular magnetic anisotropy have drawn increased attention due to their potential for higher storage densities in magnetic memory applications[1,2,3]. To fabricate such devices, one essential component, the ferromagnetic electrode, which serves as a polarized electron source, has to satisfy two criteria: 1) High value of spin polarization; 2) Magnetic easy axis points out of the film plane. The focus of most efforts has been on transition metal (TM) and heavy elements based multilayers, which are proven structures with high perpendicular magnetic anisotropy (PMA). However, concerns such as large damping due to the heavy elements and poor compatibility with the common barrier material prevent them from being realized in practical applications. For magnetic tunnel junction (MTJ) device, the recently developed ultra thin FeCoB layer with PMA offers a new route to tackle the problem, in which a high tunneling magnetoresistance (TMR) (>100%) and an easy axis perpendicular to the film plane are simultaneously realized[4]. However, the utilization of interface anisotropy that produces out-of-plane easy axis demands precise and critical control of layer thicknesses (less than 1.3 nm) and interface conditions.

Iron nitrides are known to form various phases. Much attention was focused on their saturation magnetization ($M_s$) due to the debatable claim of giant $M_s$ ($4\pi M_s \sim 3.0T$) observed on the $Fe_{16}N_2$ phase decades ago[5,6,7]. Recently, we reported the discovery of the origin of the giant saturation magnetization of such an enigmatic material[8,9]. However, the magnetic anisotropy of this material system has received less attention since most of the known iron nitride phases only possess low magnetocrystalline anisotropy (MCA).  In principle, $Fe_{16}N_2$ and its relevant Fe-N martensite form a tetragonal distorted Fe lattice As a consequence, due to the reduced crystal symmetry, a large MCA is expected to develop, given the reduced energy separation between the two orbitals $d_{x2-y2}$ and $d_{xy}$, which are located below and above the Fermi level, respectively[10]. Since its a-lattice constant (in-plane lattice constant) closely matches that of bcc Fe, this allows the epitaxial control and consequently the realization of an MCA perpendicular to thin film plane if Fe (001) substrate is provided.

Following this idea, we grew epitaxial Fe-N martensite thin films. We systematically controlled    the stoichiometry of Fe-N films using a facing-target sputtering method, which is secondary electron free from substrate with the confined plasma just between the targets[11,12,13]. A structural characterization based on x-ray diffraction (XRD) and transmission electron microscopy (TEM) imaging reveal the crystal quality and film morphology, which shows that the c-axis of the Fe-N layer is perpendicular to the film plane and is coherently adapted on the Fe(001)/GaAs(001) template. A complementary study of magnetometry and polarized neutron reflectometry show that an MCA perpendicular to the film plane is developed in the Fe-N layer. Moreover, a subsequent post-annealing process facilitates the formation of chemically-ordered $Fe_{16}N_2$ phase and further enhances the MCA, which is evaluated to exceed $10^7$ erg/cm$^3$. The combination of the large magnetocrystalline anisotropy and its giant saturation magnetization may point a new direction for the synthesis of rare-earth-element free magnets in future. In addition, we measured the spin polarization ratio of partially ordered $Fe_{16}N_2$ thin films using a Point Contact Andreev Reflection (PCAR) method[14], which shows a relatively large spin polarization ratio (P~0.52). These combining properties make the $Fe_{16}N_2$ and Fe-N martensites a promising candidate for the ferromagnetic electrodes for future spintronic devices.

## II.    Experimental and discussion

### A.  Tunable tetragonality of Fe-N maternsites

It is known that the $\alpha'$-Fe-N martensites form interstitial solid and can accommodate N concentration up to ~13 at.%[15]. In our previous study (Ref. 11), we demonstrated that with an Fe buffer layer providing (001) epitaxial constraint and allowing the increase of the $N_2$ partial pressure during Fe-N growth, it is possible to epitaxially support the Fe-N martensites with (001) texture. As schematically shown in Fig. 1a, in principle, by controlling the dopant concentration (N at. %), the c-lattice constant can be adjusted while the a-lattice is constrained by the underneath Fe buffer layer. As a result, the tetragnality can be fine-tuned. In light of these discussions, we systematically fabricated samples with Fe-N layer thicknesses in the range of 45~50 nm using a facing-target sputtering method. Prior to the growth of Fe-N layer, an Fe layer with a fixed thickness of

22 nm is deposited on GaAs (001) substrate at temperature of 250°C to encourage (001) epitaxy at an Ar pressure of 5 mTorr. The subsequent Fe-N layer is prepared by sputtering Fe targets with thoroughly mixed Ar and $N_2$ working gases (~1% $N_2$).

In Fig. 1b, the XRD peaks (measured by Philips X'Pert Pro X-ray Diffractometer with Cu Kα radiation) from Fe-N (002) showed a consistent shift towards the lower 2θ values, indicating an elongated d-spacing along the (001) direction with a typical texture deviation of 0.88° (Fig. 1c) according to the rocking curve measured on the Fe-N (002) diffraction peak. This suggests the c-lattice constant substantially enhances (>10%) as the increase of N interstitial solubility given the progressively higher $N_2$ partial pressure (Fig. 1d) used in depositing these samples.

To further examine the crystal quality and epitaxial relationship of the present films, we used high resolution (HR) transmission electron microscopy (JEOL 2200FS) (TEM) to study a cross-sectional sample that may possess the largest c-lattice constant according to the XRD. Fig. 2a shows a high-angle annular dark-field TEM image with low magnification. In addition to the GaAs substrate, Fe and Fe-N layers as outlined in the figure, Cr cap layer (~8 nm) and carbon (~1 μm) layer are deposited *ex-situ* for protection of further oxidation. The brightness contrast between two layers is clearly seen, which is due to the presence of light element N in the Fe-N layer. Aberration-corrected lattice images with nominal resolution of <0.1nm were recorded at the Fe/Fe-N interface (Fig. 2b) to reveal the epitaxy of both layers. To analyze the periodicities, a diffractogram from a 128 x 128 pixels region (i.e. region A) was computed, and the X and Y scan directions calibrated so that the diffraction spots positions closely matched the known d-spacings for the α-Fe structure, as shown in Fig. 2c. The calculated d-spacing matches with a [110] zone axis (axis that parallel to the observation direction) for both Fe and Fe-N. In addition, the in-plane direction only presents one periodicity, suggesting perfect lattice matching along that direction. Two periodicities are seen in the interface region (box A), indicating the presence of two types of d-spacing along film normal. Similar periodicity analysis in region of Fe-N layer (box B) shows an expected single d-spacing and is coherent with the longer distanced d-spacing obtained in analyzing box A. These observations demonstrate the effect of doping N atoms in the crystalline Fe causes a directional expansion of the crystal lattice along c-axis perpendicular to the film plane

while the in-plane lattice constant (a) is maintained and coherent with the Fe underlayer. The calculated d-spacing reasonably matches with that observed by XRD.

## B. Magnetic characterization of Fe-N martensites

To systematically study the magnetic properties of these films, first we investigated the in-plane M-H hysteresis loops (Fig. 3a) measured by a Princeton Measurements Vibrating Sample Magnetometer at room temperature, which clearly reveal a correlation between the saturation magnetic field ($H_s$, defined in Fig. 3b) and the average c-lattice constant as determined from XRD. The selective M-H loops (normalized to saturation magnetization) of these samples are shown in Fig. 3b. An evolution from typical easy axis to hard axis loop is expectedly seen as c-lattice constant of the Fe-N layer progressively increases, with its highest $H_s$ larger than 4 kOe, suggesting a MCA developed in the film due to the presence of Fe-N layer. However, the small but notable $M_r$ suggests the film possess both in-plane and out-plane magnetization components due to the existence of soft Fe underlayer and its strong exchange coupling with the Fe-N layer.

To facilitate the discussion of the magnetic contribution of Fe underlayer, we studied the thickness dependence of in-plane M-H loops for samples prepared at $N_2$ partial pressure of 0.12 mTorr, (deposition condition to fabricate Fe-N films with largest c/a ratio). As shown in Fig. 4a and 4b, by increasing the thickness of Fe-N layer, the saturation field saturates rapidly and levels off at around $H_s \sim 7$ kOe, suggesting the films possess a remanent (external field H=0) magnetic configuration as shown in the inset. In particular, as the thickness of Fe-N layer increases, the magnetic contributions from the underlayer (Fe) and interfacial (Fe/Fe-N) regions become progressively weak. In that case, the saturation field is determined by the crystalline anisotropy of the hard layer towards the top interface. The presence of the typical hard axis loop measured in-plane show a clear reversible magnetization rotation process, which provides the evidence of out -of-plane oriented magnetization domains in the Fe-N layer.

## C. MCA in partially ordered $Fe_{16}N_2$

Furthermore, in a previous investigation, we showed that a dramatic increase of saturation magnetization ($M_s$) was observed after in-situ post-annealing the as-deposited Fe-N films[16], which is attributed to the presence of chemically ordered $Fe_{16}N_2$ and is

associated with the increase of N site ordering (D).Here, by systematically analyzing M-H loops of optimally annealed (120 °C for 40 hrs) samples with same bilayer structure, we show that the $H_s$ also increases monotonically.

In Fig. 5a, the XRD patterns of an as-deposited and an annealed sample with the same nominal structure (Fe-N(48nm)/Fe(22nm/GaAs)) were compared. The main difference occurs at $2\theta=28.6°$, where the XRD pattern of the annealed sample develops a robust peak and can be indexed to $Fe_{16}N_2(002)$, originated from the superlattice diffraction given the alternating occupancy of N in crystalline $Fe_{16}N_2$ (inset of Fig. 5a). By analyzing the integrated intensity ratio between (002) and (004) peaks, it is possible to estimate the volume fraction of the $Fe_{16}N_2$ in Fe-N layer. To facilitate the discussion, we introduced a parameter D, which describes the degree of N ordering as shown in detail previously (Ref. 16) The in-plane M-H loops of both samples are compared in Fig. 5b. It is seen the $H_s$ increased substantially in the annealed sample. More samples with different D value are compared in Fig. 5c, in which a correlation between D and $H_s$ is clearly seen.

To further evaluate the magnetic configuration in more details, both in-plane and out-of-plane M-H loops for a partially ordered sample (D=0.32) are shown in Fig. 6a. As for the out-of-plane loop, as stated above, due to the magnetic contribution of the Fe layer, the samples develops both in-plane and out-plane magnetization components at remanence state as schematically shown in the inset of Fig. 6a. As a result, the in-plane magnetization component causes the large demagnetization linear background up to about 16 kOe in order to fully saturate the sample along the out-plane direction. However, at applied field of H~5.7 kOe, a switching is clearly seen which is originated from the magnetization flip of the out-of-plane component in the Fe-N layer. For a rough estimation, the $H_s$ measured in-plane coincides with the larger switching point measured out-of plane, suggesting the anisotropy field $H_k$ is close to $H_s$ with crystalline anisotropy ($K_u$) aligning perpendicular to film plane. Therefore, we can calculate[17] the crystalline anisotropy in the Fe-N layer as a function of N site ordering after knowing the saturation magnetization ($M_s$) of Fe-N layer (Fig. 6b). The highest $K_u$ is seen around $\sim10^7$erg/cc, which agrees well with the previous reported value determined by torque curve measurements (Ref.7). It is worth mentioning that the present synthesis process (deposition and post-annealing) does not produce phase-pure $Fe_{16}N_2$ from the structural

analysis. In particular, the highest volume fraction of the $Fe_{16}N_2$ in the Fe-N layer, which is consisted of $Fe_{16}N_2$and $Fe_8N$, has been obtained to be ~39% according to the XRD analysis using the current sputtering fabrication process. However, the increasing trend of the $K_u$ upon the degree of N ordering increases clearly shows that the MCA should be much higher for pure phase $Fe_{16}N_2$.

### D. Polarized neutron magnetometry

To confirm the magnetic configuration based on the hysteresis loop analysis, in-depth and field-dependence Polarized Neutron Reflectometry (PNR) experiments were performed using the Magnetism Reflectometer on beamline 4A at Spallation Neutron Source, Oak Ridge National Laboratory[18]. This is a time-of-flight (TOF) instrument with a wavelength band of 2–5 Å and a polarization efficiency of ~98%. When conducting the PNR experiments, an external magnetic field was applied parallel to the thin film plane. The non-spin-flip reflectivity curves of spin up and spin down neutrons were spontanously recorded. Representative fitted PNR spectra for one partially ordered sample are shown in Fig. 7a~c, in which three different in-plane fields smaller than the $H_s$ are purposely chosen after saturating the sample at around $H_s = 20$ kOe. With the nuclear scattering length density (NSLD) closely matching the nominal value (Fig. 7d), the spontaneously fitted in-plane projection of the magnetization depth profile ($M(z)_{in-plane}$) was retrieved (Fig. 7e). It is seen that in contrast to that of the Fe layer, the in-plane component of the magnetization vector $M(z)_{in-plane}$ of the Fe-N layer goes down drastically with decreasing in-plane external field. This can have two scenarios. In the first one, the Fe-N film forms in-plane nearly antiferromagnetic in-plane domains. In the second one, the film magnetization turns out-of-plane due to the out-of-plane easy-axis. The first scenario is possible only if the Fe-N film would have uniaxial in-plane anisotropy, which is not the case. In addition in the first scenario, a strong magnetic off-specular scattering would appear. However we did not record an increase in the off-specular scattering. In the second scenario, no additional off-specular scattering is expected, because the out-of-plane component of the magnetization vector is parallel to the momentum transfer Q and the in-plane parallel component contributes to the specular reflection. Hence the reduction of the in-plane magnetization originates from the evolution of the out-of plane magnetization component along the perpendicular easy

axes. It is worth mentioning that the oscillation magnitude of the R⁻ curve is relatively small comparing to R⁺. Since the oscillation magnitude is directly related to the SLD contrast between the film and the substrate. This observation is likely due to the SLD of the R⁻ is very close to that of the substrate in contrast to the SLD of R+. This effect is especially robust as it approaches the bottom interface (GaAs/Fe) interface, in which case the scattering behavior of that region is dominated by the reflectivity at high $q_z$ and consequently results in the "smearing out" of the oscillation magnitude.

### E. Spin polarization ratio measurement

Encouraged by the magnetic characterization, we performed a *direct* measurement of the transport spin-polarization (SP) using PCAR (Ref. 14 ) on a partially ordered $Fe_{16}N_2$ sample in Fig. 8. A superconducting (Nb) tip was gently pressed into the sample to minimize the effect of surface oxidation. At least 10 such different contacts were created and tested at a temperature of 1.6K. Fig. 8a and b shows normalized conductance $G(V)/G_n$ versus $V/V_\Delta$, in which $G_n$ is the conductance at applied voltage $V \gg V_\Delta$ and $V_\Delta$ is the superconducting gap of Nb. The PCAR experimental curves were fitted by the modified[19] BTK model[20] with the fitting parameters spin polarization, P, and barrier strength, Z. The superconducting gap, $\Delta$, was fixed to the value for Nb. An effective temperature (3.5K) was used to improve the quality of the fit for low Z junctions (Figure 8 (b)) suggesting that electron heating was occurring. The noise observed in the data is relatively large, which is attributed to the weak signal produced as the SP is close to 0.5. Fits based on a ballistic model reproduces the experimental data reasonably well producing an apparent dependence of P on Z. As a result, intrinsic spin polarization value was obtained by extrapolating the result to Z=0.[21] Figure 4 (c) shows the linear fit of P versus Z, which intercepts Z=0 at 0.52, namely the spin polarization of our sample approximates 52%. In comparison with reported values of ~45% on Fe samples using similar probing approaches[22], the present results show moderate enhancement.

### III. Summary

In conclusion, we have spontaneously realized perpendicular mangetocrystalline anisotropy (MCA) and high spin polarization ratio (SP) by a simple scheme, namely, tuning the c-lattice constant of bcc Fe by interstitial doping of N. The in-plane lattice

parameter of the present Fe-N films is close to bcc Fe, allowing a direct epitaxial adaption with a MgO barrier for MTJ and a Ag spacer for GMR applications. Furthermore, utilizing light-element (e. g. B, C, N) and ferromagnetic (e. g. Fe, Co, Ni) interstitial alloys to develop magnetic material with strong perpendicular MCA without using any *rare earth* elements offers promising approaches of searching and identifying new magnet materials for clean energy applications.

## Acknowledgement

† email: jpwang@umn.edu

**Figure Captions**

FIG. 1 (a) A sketch of different stages of Fe-N tetragonality (c/a) due to the N interstitial doping. (b) XRD of as-deposited Fe-N martensite thin films with different c-lattice constant. Data from different samples are consistently vertically shifted by a factor of 10 in log scale. The substantial horizontal shift of Fe-N (002) diffraction peak (labeled by arrows) is due to the different $N_2$ partial pressure used in the growth of each sample. (c) Rocking curve measured on Fe-N (002) peak of the sample with largest c-lattice constant. (d) c-lattice constant calculated from XRD in (b) as a function of $N_2$ partial pressure in the growth of each sample (all other deposition conditions are kept the same).

FIG. 2 (a) Low-mag HAADF image of a cross-section epitaixial Fe-N martensite thin film. The layered structure at the top interface is due to the Cr and C capping as described in the text. (b) A zoom-in look of the lattice image acquired at the Fe/Fe-N interface (outlined as a box in (a)) with a [110] zone axis. The images with in the boxes labeled as A and B are processed by diffractogram as shown correspondingly in (c) and (d). A clear "double peak" is shown in A (highlighted by yellow arrows) corresponding to the lattice periodicity from Fe and Fe-N, respectively. Only one type of lattice periodicity is shown in (d), corresponding to only one d-spacing in Fe-N layer.

FIG. 3 (a) In-plane saturation field ($H_s$) as a function of c-lattice constant according to XRD results in FIG. 1. (b) Selective M-H loops measured in-plane for samples labeled A-D in accordance with that presented in (a). The magnetic field of the point as marked by the arrow in C is the saturation field ($H_s$) defined in this study.

FIG. 4 (a) In-plane saturation field ($H_s$) as a function of thickness of Fe-N layer with same tetragonality (c/a). Inset shows the schematic drawing of magnetization configuration at remanence as explained in the text. (b) Selective M-H loops measured in-plane for samples with different Fe-N layer thickness as outlined in each figure.

FIG. 5 (a) X-ray diffraction pattern of as-deposited and annealed samples with similar structure (Fe-N(48nm)/Fe(22nm)GaAs). The inset shows the crystal unite cell of $Fe_{16}N_2$. The ordered site occupation of the N atoms causes the diffraction of $Fe_{16}N_2$(002), which is not seen in as-deposited sample. (b) M-H loops measured in-plane for the two samples shown in (a). (c) in-plane saturation field ($H_s$) as a function of N site ordering D as defined in Ref. 12.

FIG. 6 (a) In-plane (solid) and Out-of-plane (dash) M-H loops measured on one partially ordered $Fe_{16}N_2$ sample (D~0.32). The Fe-N layer switches at Hc~5.7kOe (black arrows). (b) Calculated $K_u$ as a function of degree of N site ordering (D) in partially ordered $Fe_{16}N_2$ thin film samples as described in text. The dashed line here is a guide to the eye. All the samples have the same nominal thickness structure: Fe-N(48nm)/Fe (22nm)/GaAs.

FIG. 7 (a)~(c) fitted polarized neutron with spin-up (R+) and spin-down (R-) reflectivity curves for an annealed sample at external field of 5, 50, and 200 mT. (d) Nuclear scattering length density and (e) field dependent in-plane magnetization depth profiles as functions from the distance from the substrate

FIG. 8 PCAR measurement on partially ordered $Fe_{16}N_2$ with structure Fe-N(48nm)/Fe(22nm)/GaAs. (a) and (b) Normalized conductance as a function of applied voltage (V) divided by superconducting gap ($V_\Delta$). Experimental data is shown in dots (green) and fitting is shown in continues curve (red), (c) Spin Polarization as a function of Z (described in text), the experiment data (green dots) is fitted linearly (straight line).
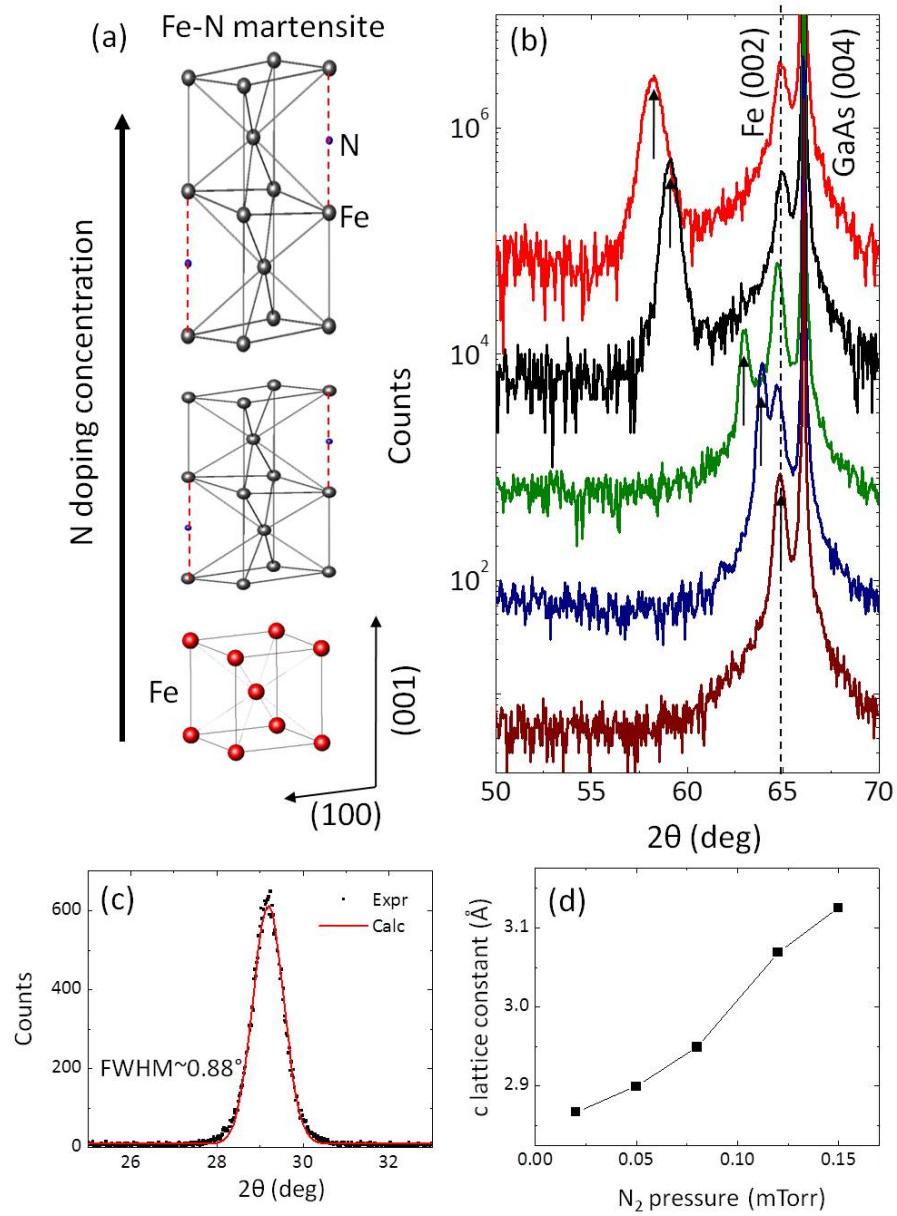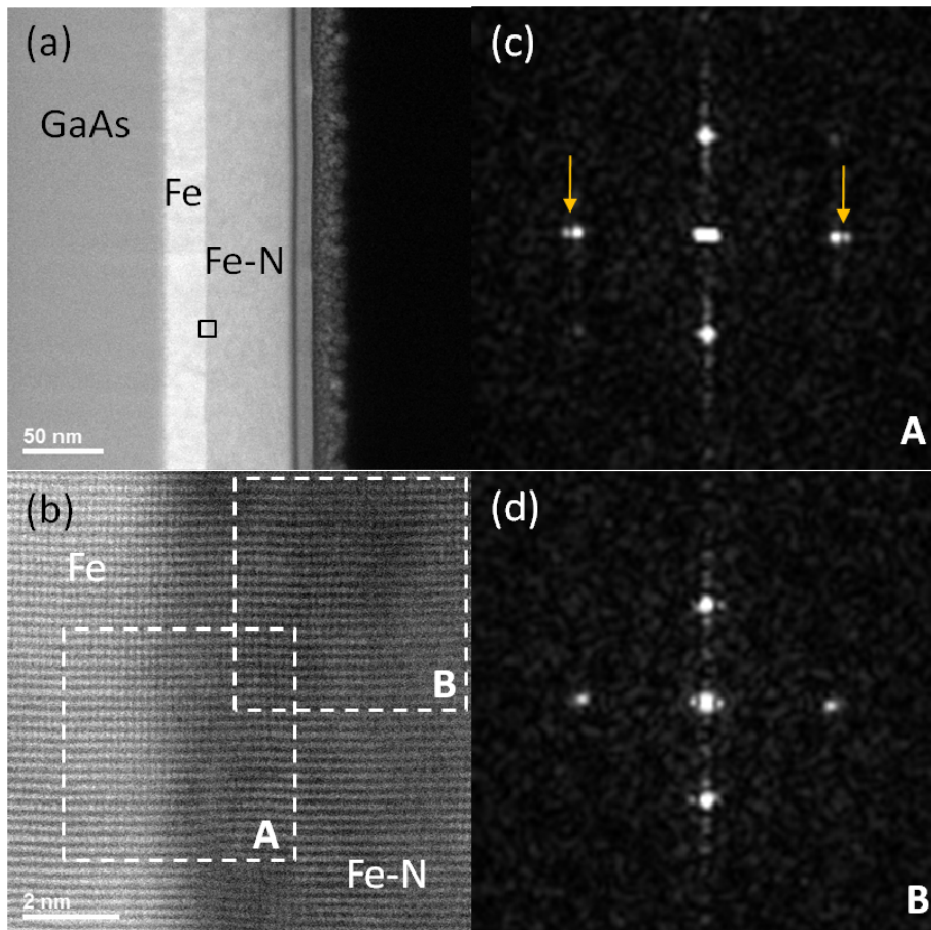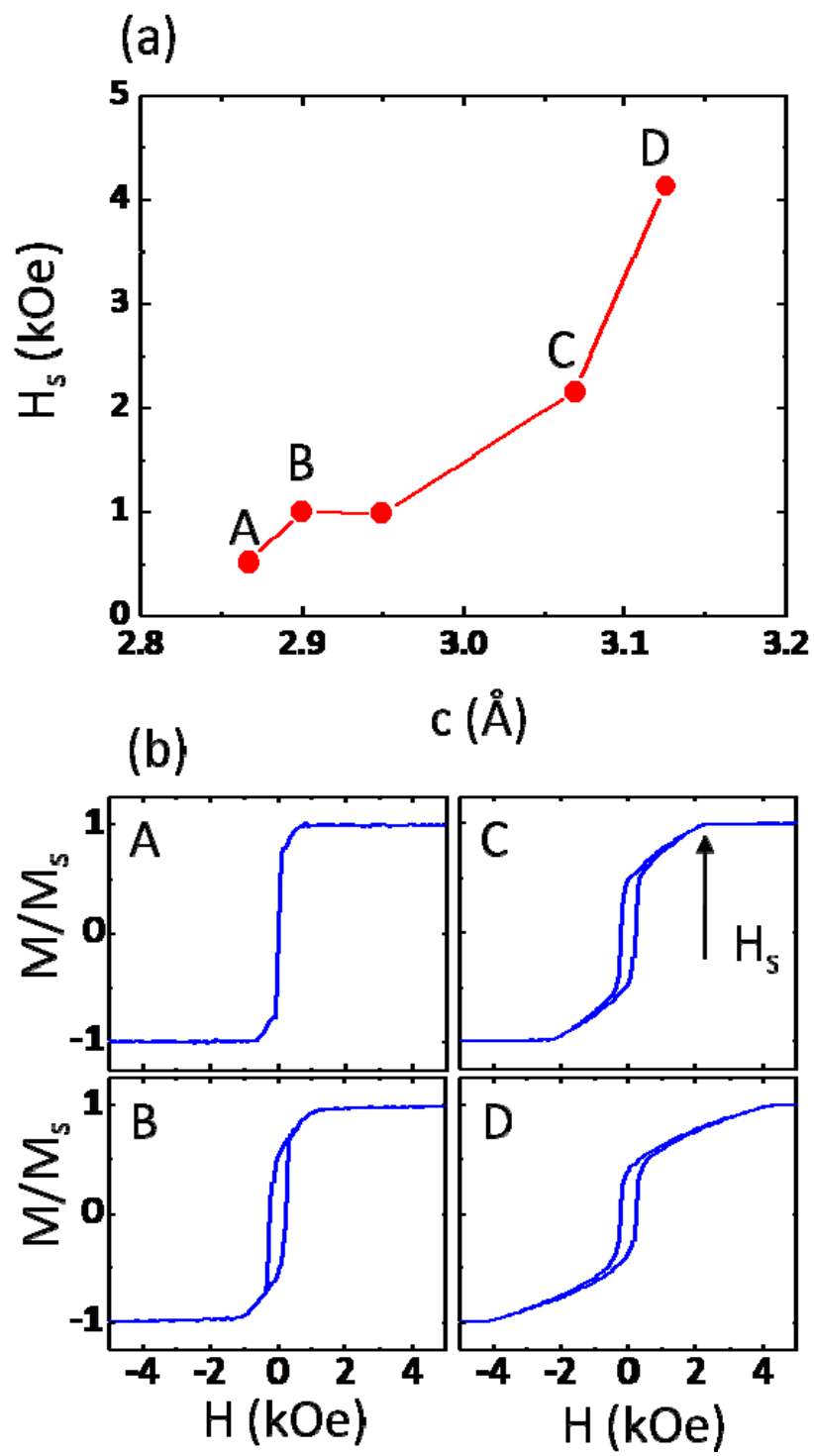
FIG. 1



(a) Fe-N martensite
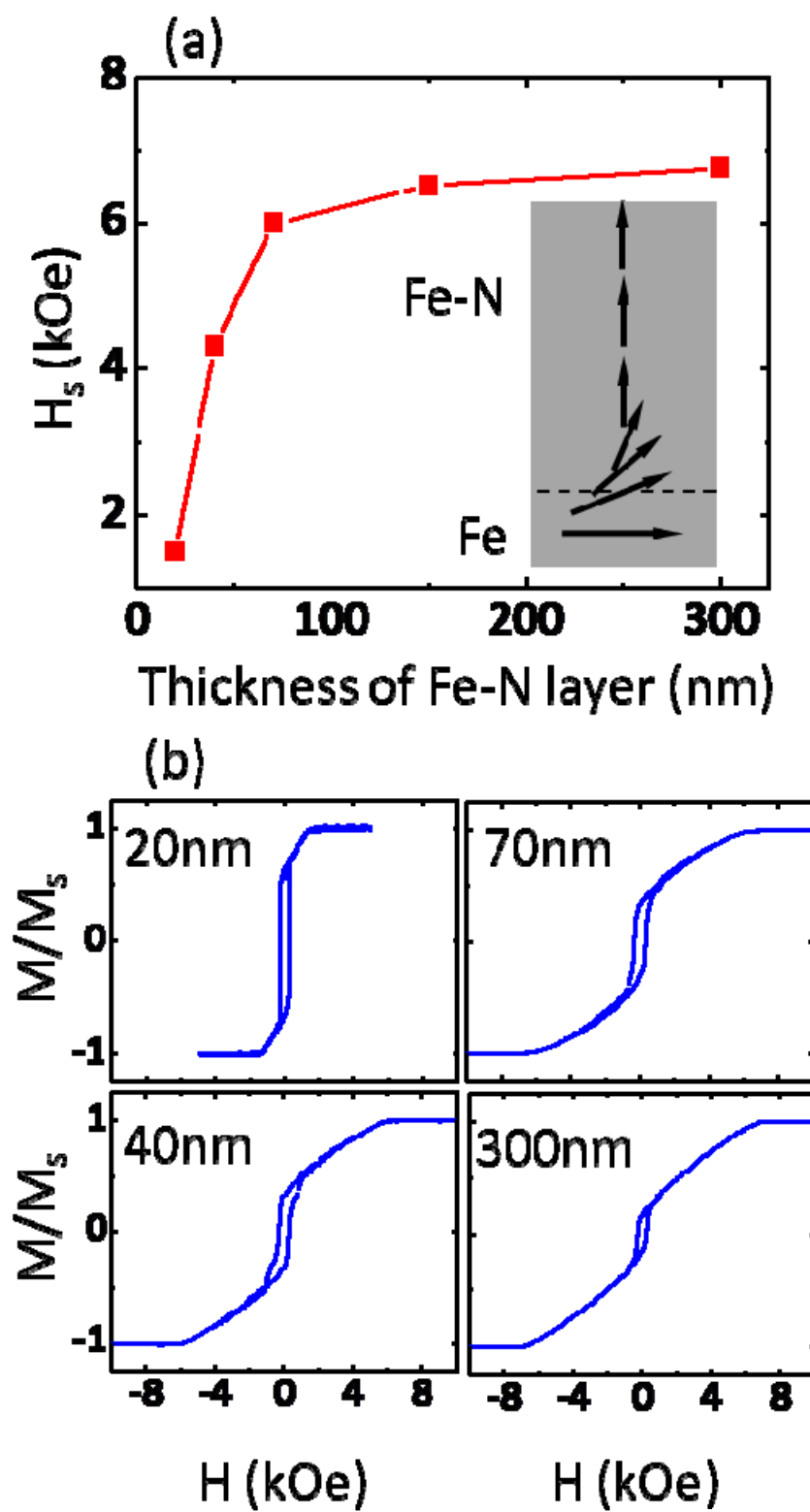
N doping concentration

N
Fe

Fe

(001)

(100)

(b) Fe (002)  GaAs (004)

Counts

$10^6$

$10^4$

$10^2$

50    55    60    65    70

2θ (deg)

(c)

Counts

600

400

200    FWHM~0.88°

0

26    28    30    32

2θ (deg)

• Expr
— Calc

(d)

c lattice constant (Å)

3.1

3.0

2.9

0.00    0.05    0.10    0.15

N₂ pressure (mTorr)

FIG. 2

FIG. 3



(a)

(b)

FIG. 4

FIG. 5



(a) X-ray diffraction patterns for as-deposited (blue) and post-annealed (red) samples, showing peaks labeled Fe$_{16}$N$_2$ (002), GaAs (002), Fe$_{16}$N$_2$ (004), Fe (002), and GaAs (004), with an inset crystal structure showing Fe and N atoms.

(b) Magnetization hysteresis loops, $4\pi M$ (Tesla) versus $H$ (kOe), for post-annealed (red) and as-deposited (gray) samples.

(c) $H_s$ (kOe) versus $D$ (N site ordering).
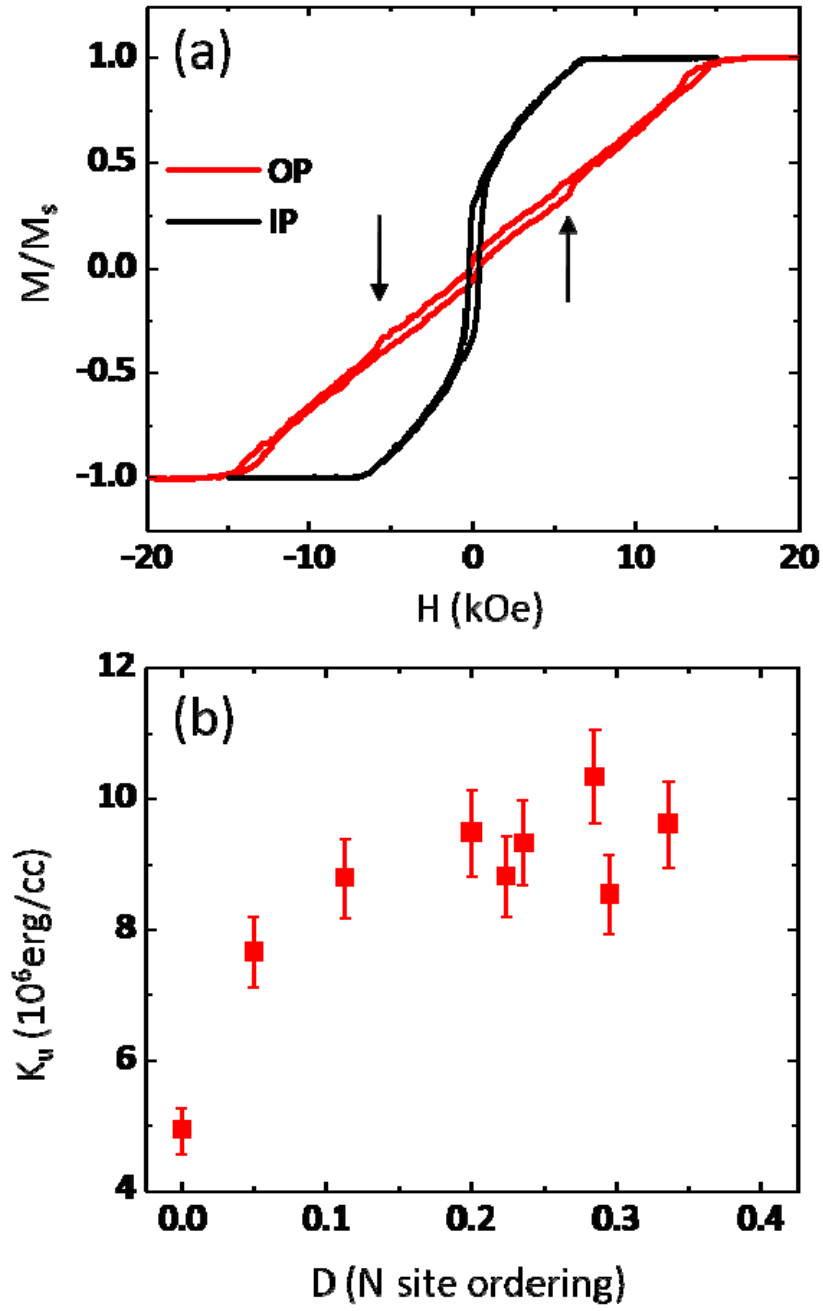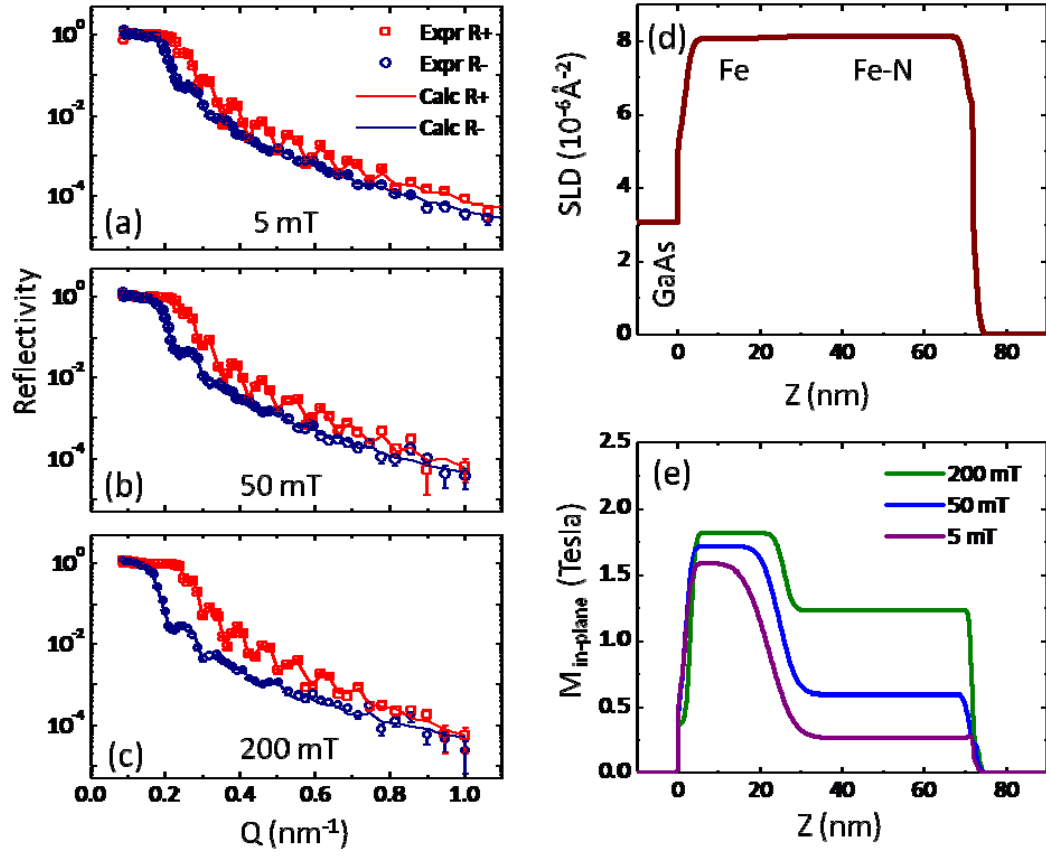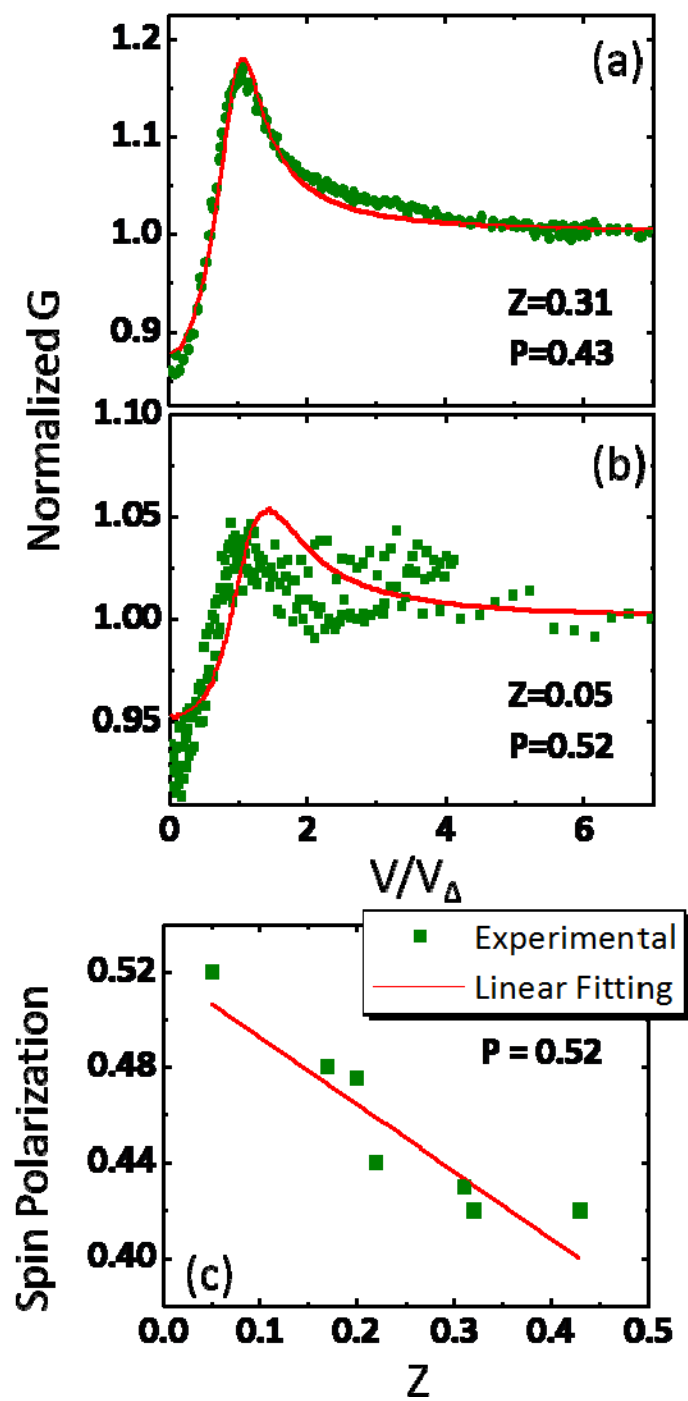
FIG. 6

FIG. 7

FIG. 8

## References

[1] H. Meng and J.-P. Wang, *Appl. Phys. Lett.* **88**, 172506 (2006)

[2] S. Mangin, D. Ravelosona1, J. A. Katine, M. J. Carey, B. D. Terris and Eric E. Fullerton, *Nat. Mater.* **5**, 210 (2006).

[3] T. Seki, S. Mitani, K. Yakushiji, and K. Takanashi, *Appl. Phys. Lett.* **88**, 172504 (2006).

[4] S. Ikeda, K. Miura, H. Yamamoto, K. Mizunuma, H. D. Gan, M. Endo, S. Kanai, J. Hayakawa, F. Matsukura and H. Ohno, *Nat. Mater.* **9**, 721 (2010)

[5] T. K. Kim and M. Takahashi, *Appl. Phys. Lett.* **20** (12), 492 (1972); Y. Sugita, K. Mitsuoka, M. Komuro, H. Hoshiya, Y. Kozono, and M. Hanazono, *J. Appl. Phys.* **70** (10), 5977 (1991); M. Takahashi, H. Shoji, H. Takahashi, H. Nashi, T. Wakiyama, M. Doi, and M. Matsui, J Appl. Phys. 76 (10), 6642 (1994)

[6] At the annual conference on Magnetism and Magnetic Materials in 1996, a symposium was held on the topic $Fe_{16}N_2$, on which both theorists and experimentalists presented their work. The papers were published in J. Appl. Phys. **79** 5564-5581 (1996). No decisive conclusion was drawn on whether it has giant saturation magnetization. This has been mainly due to the lack of a convincing theory and unavailability of repeatable samples. This topic has been largely dropped by the research community of magnetic materials and magnetism since then.

[7] H. Takahashi, M. Igarashi, A. Kaneko, H. Miyajima, Y. Sugita,, *IEEE Trans. Magn..* **35** (5), 2982 (1999).

[8] N. Ji, X. Liu and J.-P. Wang, *New J. Phys.* **12** (6), 063032 (2010).

[9] X. Liu, Y.-H. Xu, C. Sanchez-Hanke, J.-P. Wang arxiv: 0909.4478

[10] P. Bruno, *Phys. Rev. B* **39**, 865 (1989).

[11] N. Ji, Y. Wu, and J.-P. Wang, *J. Appl. Phys.* **109**, 07B767 (2011)

[12] J. R. Shi and J. P. Wang, *Thin Solid Films*, 420, 172 (2002)

[13] Z. H. Qian, Geng Wang, J. M. Sivertsen, J. H. Judy; *IEEE Trans. Magn.,* 33, 3748 (1997)

[14] R. J. Soulen, Jr., J. M. Byers, M. S. Osofsky, B. Nadgorny, T. Ambrose, S. F. Cheng, P. R. Broussard, C. T. Tanaka, J. Nowak, J. S. Moodera, A. Barry and J. M. D. Coey,

*Science* **282** 85 (1998)

[15] K. H. Jack, *Proc. R. Soc. London. Ser.* A **208** 200 (1951)

[16] N. Ji, L. F. Allard, E. Lara-Curzio, and J.-P. Wang, *Appl. Phys. Lett.* **98**, 092506 (2011)

[17] To calculate the $K_u$, we used the equation: $K_u=H_k*M_s/2$, where $M_s$ is the saturation magnetization of the Fe-N layer and $H_k$ is $H_s$ as defined in text.

[18] V. Lauter, H. Ambaye, R. Goyette, W.-T. H. Lee, A. Parizzi, *Physica B* **404**, 2543 (2009); V. Lauter-Pasyuk, *J. Phys. IV France 1* (2007); V. Lauter-Pasyuk, H. J. Lauter, B. P. Toperverg, L. Romashev, and V. Ustinov, *Phys. Rev. Lett. 89, 167203* (2002)

[19] I. I. Mazin, A. A. Golubov, and B. Nadgorny, *J. Appl. Phys. 89, 7576 (2001)*; G. T. Woods, R. J. Soulen, Jr., I. Mazin, B. Nadgorny, M. S. Osofsky, J. Sanders, H. Srikanth, W. F. Egelhoff, and R. Datla, *Phys. Rev. B* **70**, 054416 (2004).

[20] G. E. Blonder, M. Tinkham, and T. M. Klapwijk, *Phys. Rev. B* 25, 4515 (1982).

[21] Y. Ji, C. L. Chien, Y. Tomioka, and Y. Tokura, *Phys. Rev. B* **66**, 012410 (2002); Y. Ji, G. J. Strijkers, F. Y. Yang, C. L. Chien, J. M. Byers, A. Anguelouch, G. Xiao, and A. Gupta, *Phys. Rev. Lett.* **86**, 5585 (2001); P. Raychaudhuri, A. P. Mackenzie, J. W. Reiner, and M. R. Beasley, *Phys. Rev. B* **67**, 020411 (2003); C. H. Kant, O. Kurnosikov, A. T. Filip, P. LeClair, H. J. M. Swagten, and W. J. M. de Jonge, *Phys. Rev. B* **66**, 212403 (2002).

[22] B. Nadgorny, R. J. Soulen, Jr., M. S. Osofsky, I. I. Mazin, G. Laprade, R. J. M. van de Veerdonk, A. A. Smits, S. F. Cheng, E. F. Skelton, and S. B. Qadri , *Phys. Rev. B* **61**, R3788 (2000).